Photodiagnosis and Photodynamic Therapy 28 (2019) 125–131

Contents lists available at ScienceDirect

Photodiagnosis and Photodynamic Therapy

journal homepage: www.elsevier.com/locate/pdpdt

Photoexcitation triggering via semiconductor Graphene Quantum Dots by photochemical doping with Curcumin versus perio-pathogens mixed biofilms

Maryam Pourhajibagher[a], Steven Parker[b], Nasim Chiniforush[c], Abbas Bahador[d,*]

[a] Dental Research Center, Dentistry Research Institute, Tehran University of Medical Sciences, Tehran, Iran
[b] Department of Surgical Sciences and Integrated Diagnostics, University of Genoa, Italy
[c] Laser Research Center of Dentistry, Dentistry Research Institute, Tehran University of Medical Sciences, Tehran, Iran
[d] Oral Microbiology Laboratory, Department of Medical Microbiology, School of Medicine, Tehran University of Medical Sciences, Tehran, Iran

ARTICLE INFO

Keywords:
Graphene Quantum Dot
Curcumin
Antimicrobial photodynamic therapy
Periodontitis
Peri-implantitis

ABSTRACT

Background: Recently, antimicrobial photodynamic therapy (aPDT) as an alternative treatment modality has been used adjunctively in the treatment of periodontitis and peri-implantitis. Photosensitizing agents in the form of nanoparticles have been designed for improving the efficiency of aPTD. Graphene quantum dots are a special type of nanocrystals that can promote aPDT when coupled with curcumin (Cur). The main objective of the present study was to investigate the effects of photoexcited GQD-Cur on the metabolic activity of perio-pathogen mixed biofilms.

Materials and methods: GQD-Cur was synthesized and characterized by scanning electron microscopy (SEM), dynamic light scattering (DLS), fourier transform infrared (FTIR) spectroscopy, ultraviolet-visible spectrometry (UV–Vis), and X-ray diffraction (XRD). The cell cytotoxicity effect of GQD-Cur was evaluated on primary human gingival fibroblast (HuGu) cells. Perio-pathogen mixed biofilms including *Aggregatibacter actinomycetemcomitans*, *Porphyromonas gingivalis*, and *Prevotella intermedia* photosensitized with GQD doped with Cur were irradiated with a blue LED at a wavelength of 435 ± 20 nm for 1 min, and then bacterial viability measurements were performed. The antimicrobial susceptibility profile, biofilm formation ability, amount of reactive oxygen species (ROS) released, and variations of gene expressions involved in biofilm formation were assessed.

Results: The SEM, DLS, FTIR, UV–Vis spectrometry, and XRD pattern confirmed that GQD-Cur was synthesized successfully. According to the results, GQD-Cur exhibited no cytotoxicity against HuGu cells. Photoexcited GQD-Cur resulted in a significant reduction in cell viability (93%) and biofilm formation capacity (76%) of peri-pathogens compared to the control group ($P < 0.05$). According to the results, a significant concentration-dependent increase in the ROS generation was observed in perio-pathogens mixed cells treated with different doses of GQD-Cur-aPDT. Moreover, *rcpA*, *fimA*, and *inpA* gene expression profiles were downregulated by 8.1-, 9.6-, and 11.8-folds, respectively.

Conclusions: Based on the results, photoexcited GQD-Cur have a high potency of perio-pathogens suppression in planktonic and biofilm forms and downregulation of the biofilm genes expression pattern was exploited as a nanoscale-based platform for periodontitis.

1. Introduction

Periodontal diseases are polymicrobial inflammatory/ infectious diseases that can damage the periodontal ligament, adjacent supportive alveolar bone, and periodontal tissues supporting the teeth [1]. It is recognized that some anaerobic Gram-negative perio-pathogen bacteria in the subgingival plaque biofilm, including *Aggregatibacter actinomycetemcomitans*, *Porphyromonas gingivalis*, and *Prevotella intermedia,* play a key role in the initiation/progression of periodontitis [2,3].

The main purpose of most therapeutic modalities for the treatment of periodontitis is the elimination of perio-pathogen microorganisms and restoration of the lost form and function of the periodontium [4]. Successful treatment of periodontal defects is greatly related to the

* Corresponding author at: Oral Microbiology Laboratory, Department of Microbiology, Tehran University of Medical Sciences, Tehran, Iran.
E-mail address: abahador@sina.tums.ac.ir (A. Bahador).

https://doi.org/10.1016/j.pdpdt.2019.08.025
Received 4 December 2018; Received in revised form 14 August 2019; Accepted 20 August 2019
Available online 31 August 2019

control of perio-pathogen microorganisms, which is achieved by removing the plaque and calculus from the tooth using manual and ultrasonic instruments [5]. However, complete removal of perio-pathogens may not be obtained with conventional mechanical or non-surgical periodontal treatments, and a supplementary therapy approach for the removal of perio-pathogens from periodontal pockets is considered essential [4].

In search of natural antimicrobial agents for treatment of local infections, many different hydrophobic agents such as curcumin (Cur), a yellow pigment extracted from turmeric (*Curcuma longa Linn*), have been found to be highly effective against various microbial pathogens [6]. The safety of Cur has been evaluated by clinical trials in humans. Cur has a broad absorption peak in the range of 300–500 nm (maximum at 430 nm), and it exhibits extended antimicrobial effects at low doses in combination with blue light-emitting diode (LED) exposure in antimicrobial photodynamic therapy (aPDT) [7–11]. It has been proven that aPDT, as an adjunct procedure, can kill microbial cells via the formation of reactive oxygen species (ROS) in the presence of a low power light with an appropriate wavelength along with a photosensitizer substance and oxygen molecules [12–14]. aPDT provides more advantages over other antimicrobial procedures, showing effectiveness against multi-drug resistant (MDR) bacteria, as it is equally effective in killing MDR microbial strains as naive strains and that microorganisms cannot readily develop drug-resistance to aPDT [15,16].

The clinical application of Cur in aPDT is complicated by its rapid hydrolysis under alkaline conditions and its low solubility in aqueous media at physiological pH. However, these drawbacks can be addressed through the modification and synthesis of various derivatives related to Cur such as encapsulation and interactions with nanoparticles including semiconductor-graphene quantum dot (GQD) [17].

GQD (less than 10 nm in size) is a class of carbon nanoparticles that has received considerable attention due to several properties such as a high specific surface area, amenability to modification, excellent solubility, favorable biocompatibility with low cytotoxicity, improved multifunctionality, high photostability, and high drug delivery [18,19]. A previous study found that GQD could absorb visible light and become activated, and then generate ROS, which is a known antimicrobial agent in phototherapy against bacteria due to photodynamic disruption of the bacterial cell membrane integrity [20]. Recently it has been shown that photoexcited GQD with blue LED (465–475 nm, 1 W) can exhibit a higher antimicrobial activity against *Escherichia coli* and *Staphylococcus aureus* [21]. Dong et al. demonstrated the synergistic photoactivated antimicrobial effects of carbon-QD in combination with photosensitizers methylene blue or toluidine blue against *E. coli* with visible light illumination [22]. Such synergistic effects may provide more effective strategies as antimicrobial methods.

Recently, the effectiveness of graphene-derivative-based drug nanocomposites (i.e. GQD-Cur) has been demonstrated for cancer therapy using GQD as a nano-vector to deliver Cur. In GQD-Cur composites, Cur was attached to the GQD by direct interactions with oxygen-containing functional groups on the surface of GQD [17]. It was hypothesized that the increase in the amount of oxygen-containing functional groups on the surface of GQD would effectively increase interactions with hydrophobic Cur, resulting in assisting in the formation of GQD-Cur composites with increased activity of Cur. Some et al. found that GQD had an ultrahigh drug-loading capacity (about 40,000 mg/g) and prolonged drug release due to the presence of a large surface area with many oxygen-containing functional groups, which is the highest value ever found for a nanomaterial-based carrier [17].

To overcome the above drawbacks of Cur-aPDT and to achieve high antimicrobial effects without using too high concentrations of Cur, a feasible strategy may be to use GQD-Cur-aPDT. The purpose of our study was to investigate whether GQD-Cur could achieve significant antimicrobial effects in deactivation of a mixed-species biofilm model of *A. actinomycetemcomitans*, *P. gingivalis*, and *P. intermedia,* as the etiological agents of periodontitis, under blue LED illumination as a new disinfection method. The growth, metabolic activity, and virulence genes expression of perio-pathogens mixed biofilms were evaluated following GQD-Cur-aPDT.

2. Materials and methods

2.1. Synthesis of graphene oxide (GO) and GQD

GO was synthesized using the modified Hummers method according to a previous study in order to prepare GQD [23]. Briefly, flake graphite was added to $NaNO_3$ (Merck, Darmstadt, Germany) and 98% H_2SO_4 (Merck, Darmstadt, Germany). $KMnO_4$ (Merck, Darmstadt, Germany) was then slowly added, and the reaction mixture was stirred at 35 °C overnight. The reaction mixture was then diluted with deionized water. For reaction termination, dH_2O_2 aqueous solution (Merck, Darmstadt, Germany) was added to the mixture. Eventually, the mixture was dialyzed to obtain purified GO.

GQD was fabricated by GO using $KMnO_4$ as previously described [24]. Briefly, GO and $KMnO_4$ were mixed and treated under microwave irradiation. Next, the mixture was centrifuged and the supernatant containing GQD was collected. The supernatant solution was then filtered (0.45 μm pore size) and dialyzed. Finally, solid GQD was obtained using incubation of the solution in an oven at 160 °C.

2.2. Synthesis of GQD-Cur as a photosensitizing agent

GQD-Cur was synthesized as described previously [17]. Briefly, GQD was dispersed in dH_2O_2 (pH 9). Then, five times the amount of Cur (Merck, Darmstadt, Germany) was added to GQD suspension dropwise. Finally, the obtained GQD-Cur suspension was centrifuged and washed with dH_2O_2, and the resulting pellet was dried under vacuum conditions.

2.3. Characterization of synthetized GQD-Cur

The morphology and microstructure of GQD-Cur was determined by scanning electron microscope (SEM) micrographs. The particle diameter of GQD-Cur was measured by dynamic light scattering (DLS) using a Malvern Zetasizer Nano ZS system at 25.2 °C. To analyze the chemical structure and bond formation, fourier transform infrared (FTIR) spectroscopy (Thermo Fisher Scientific, Massachusetts, US) with the KBr pellet method was performed. An ultraviolet–visible (UV–Vis) spectrophotometer was used to investigate the absorbance of the GQD-Cur solutions. Moreover, X-ray diffraction (XRD) patterns were collected on the X'Pert PRO MPD (PANalytical Co., Netherlands) with Cu-K (alpha) radiation and a generator setting of 40 mA and 40 Kv.

2.4. Cytotoxicity effect of GQD-Cur on human gingival fibroblast cells

Primary human gingival fibroblast cells (HuGu; IBRC C10459) were obtained from the Iranian Biological Resource Center (Tehran, Iran) and cultured in Dulbecco's Modified Eagle's Medium (DMEM, HiMedia Labs, India) supplemented with 10% fetal bovine serum (FBS; Sigma-Aldrich, United Kingdom), L-glutamine (2 mM), 1% penicillin/streptomycin antibiotic solution (10,000 Unit/mL penicillin, 10 mg/mL streptomycin), and 100 μg/mL amphotericin B, and maintained at 37 °C in a humidified atmosphere with 5% CO_2. The medium was renewed every 72 h. In the third subculture, a seeding density of 10^4 cells per well was placed in a flat-bottomed 96-well polystyrene cell culture microplate (Greiner Bio-One, Germany) and incubated with GQD-Cur (100 μg/Ml final concentration) for 24 h. After incubation, the cells were washed with sterile phosphate buffered saline (PBS) to remove non-adherent cells and media. Finally, the cell cytotoxicity was determined using a 3-(4,5-dimethylthiazol-2-yl)-2,5-diphenyltetrazolium bromide (MTT) assay kit (Sigma-Aldrich, United Kingdom) at 570 nm

according to the manufacturer's instructions.

2.5. Light source

A blue LED (DY400-4, Denjoy Dental Co., Ltd., Shenzhen, China) at a wavelength of 435 ± 20 nm with an output intensity of 1000–1400 mW/cm^2 was used as a light source. The output powers were measured by a power meter (LaserPoint s.r.l, Milan, Italy) during the experiment.

2.6. Bacterial strains and growth conditions

A. actinomycetemcomitans ATCC 33384, *P. gingivalis* ATCC 33277, and *P. intermedia* ATCC 49046 strains were cultured in anaerobic conditions for 72 h at 37 °C in a culture medium that was prepared using brain heart infusion (BHI) agar (Merck, Darmstadt, Germany) to which the following compounds were added: 5% defibrinated sheep blood (Sigma-Aldrich, United Kingdom), 5 g/L yeast extract (Merck, Darmstadt, Germany), 5 mg/L hemin and 1 mg/L menadione (both purchased from Sigma-Aldrich, United Kingdom). For preparing the bacterial suspensions, fresh BHI bacterial cultures were equally diluted in BHI broth (Merck, Darmstadt, Germany) in an optical density approximately 1.0×10^6 colony forming units (CFU)/mL, as verified by colony counting.

2.7. Evaluation of GQD-Cur effects on perio-pathogens mixed biofilms

The effect of GQD-Cur was investigated on the planktonic and biofilm forms of perio-pathogens mixed biofilms. The experimental groups were treated in accordance with the following experimental conditions:

A: Perio-pathogens mixed biofilms + GQD
B: Perio-pathogens mixed biofilms + Cur
C: Perio-pathogens mixed biofilms + GQD-Cur
D: Perio-pathogens mixed biofilms + blue LED
E: Perio-pathogens mixed biofilms + GQD + blue LED
F: Perio-pathogens mixed biofilms + Cur + blue LED
G: Perio-pathogens mixed biofilms + GQD-Cur + blue LED
H: Perio-pathogens mixed biofilms only as a control group

2.7.1. Microbial viability assay

The wells of a 96-well round bottomed sterile polystyrene microplate (TPP; Trasadingen, Switzerland) were filled with 100 µL mixed perio-pathogens at a concentration of 1.5×10^8 CFU/mL. In groups A, B, and C, 100 µL GQD (100 µg/mL final concentration), 100 µL Cur (40 µM), and 100 µL GQD-Cur (100 µg/mL final concentration) was added into the wells, respectively. The microplate was incubated in the dark at room temperature for 5 min in an anaerobic atmosphere. In group D, mixed perio-pathogens were exposed to a blue LED irradiation at a wavelength of 435 ± 20 nm for 1 min (60–80 J/cm^2). Groups E, F, and G were treated with GQD, Cur, and GQD-Cur similar to groups A, B, and C, respectively. Then, the wells were exposed to blue LED similar to group D. Mixed perio-pathogens (group H) without any treatment (photosensitizers and light) were used as a control group. After treatment, the samples were serially diluted and plated on BHI agar media enriched with the compounds mentioned above and incubated at 37 °C. The number of colonies in each sample was counted after 48 h according to a previous study [26].

2.7.2. Biofilm biomass quantification

Biofilm biomass quantification of mixed perio-pathogens was done according to a previous study [6]. Briefly, after incubation of 1.5×10^8 CFU/mL of mixed perio-pathogens in a flat-bottomed sterile polystyrene microplate (TPP; Trasadingen, Switzerland) for 48 h, the wells were treated in accordance with the treatments mentioned above. Afterward, the plates were gently washed with PBS, stained with 0.1% (wt/vol) crystal violet, and de-stained with ethanol (96%). The wells were then filled with 33% (vol/vol) acetic acid and biofilm degradation was evaluated by measuring the absorbance of the solution at 570 nm using a microplate reader (Thermo Fisher Scientific, US).

2.8. Intracellular measurement of ROS

In order to determine the induction effect of GQD-Cur-aPDT on intracellular ROS production in *E. faecalis*, different concentrations of GQD-Cur in combination with blue LED at various power densities were tested by the checkerboard method as follows.

At first, for preparation of DCFH-DA treated bacterial cultures, a combination of *A. actinomycetemcomitans*, *P. gingivalis*, and *P. intermedia* was cultured simultaneously to 1.0×10^8 CFU/mL and washed three times with PBS at pH 7.4 and re-suspended in PBS by adjusting the cell density to 10^7 CFU/mL. In the sterile microtubes, 2′,7′-dichlorfluorescein-diacetate (DCFH-DA) fluorescent probe [25] was added to the cultures at a ratio of 1 : 2000 and the mixtures were shaken at 37 °C for 10 min. The cells were then centrifuged at 10,000 rpm for 15 min and the pellets were washed twice with PBS to remove the DCFH outside the cells.

The checkerboard panel in the microplates was prepared by pipetting 100 u L dH_2O to each well; 100 u L GQD-Cur solution (0.2 mg/mL) was added to the wells in column 1 (far left of the plate) and the GQD-Cur concentration was diluted to 1:2 (i.e., 0.1 mg/mL). GQD-Cur was diluted two-fold by transferring 100 u L aliquots from column 1 to column 2. Therefore, column 2 was a two-fold dilution of column 1 (i.e., 0.05 mg/mL). The procedure was repeated down across the microplate to column 5 and then 100 u L was discarded from column 5 rather than dispensing it into column 6. Starting from column 6 to column 1, the columns were inoculated with the DCFH-DA treated bacterial cultures (100 u L/well; final concentration: 5×10^5 CFU/mL). The concentrations of GQD-Cur were ranged from 0.1 mg/mL (column 1) to 6.25 ug/mL (column 5). Column 6 contained non-treated growth control. Next, the plates were incubated in the dark for 5 min, followed by separate irradiation of each column of a 96-well plate with a blue LED at 60–80, 120–168, 180–240, 252–336, and 300–420 J/cm^2, while the control (column 6) was left untreated. The fluorescence intensity of 2′,7′-dichlorofluoroscein (DCF), as the oxidized product of hydrolyzed DCFH-DA by intracellular esterases, was measured by a fluorescence spectrophotometer at an excitation wavelength of 488 nm and at an emission wavelength of 535.

2.9. Quantitative real-time PCR (qRT-PCR) condition and genes expression analysis

After treatment of perio-pathogens mixed biofilms, which was determined according to the methods mentioned in the previous section, the total RNA of treated and control groups was extracted using an RNA extraction kit (mRNA-ONLY™ Prokaryotic mRNA Isolation Kit; Epicentre, an Illumina company, USA) in accordance with the manufacturer's instructions. The RNA concentration and quality were ascertained by NanoDrop® ND-1000 spectrophotometer (Thermo Fisher Scientific, US) using A_{260}/A_{280} and A_{260}/A_{230} ratios. The extracted RNAs were treated with RNase-free DNase I (Thermo Scientific GmbH, Germany) to eliminate the genomic DNAs and the complementary DNA (cDNA) was synthesized by the RevertAid First Strand cDNA Synthesis Kit (Thermo Fisher Scientific, US) based on the manufacturer's protocol.

qRT-PCR reactions were carried out in triplicate and run on the Line-GeneK Real-Time PCR Detection System (Bioer Technology, Hangzhou, China). The primers used in this procedure that were designed using the Primer3 v. 4.0 (http://frodo.wi.mit.edu/primer3/) are shown in Table 1. Thermal cycling conditions were 95 °C for 5 min followed by 35 cycles at 95 °C for 15 s, 55 °C for 10 s, and 72 °C for 10 s, and a final extension at 72 °C for 2 min. The expression levels of target genes were analyzed using the Livak and Schmittgen method [5].

Table 1
The primer sequences used in this study.

Microorganisms	Genes	Primer sequence (5' to 3')	Amplicon size (bp)
A. actinomycetemcomitans	*rcpA*-F	TGGGCATTAACTGGAGCCAC	72
	rcpA-R	ATCCACCTCCGAAACCGAAG	
	16S rRNA-F	AAGCACCGGCTAACTCCGT	63
	16S rRNA-R	TTCCGATTAACGCTCGCAC	
P. gingivalis	*fimA*-F	CGGAACGAATAACCCAGAGA	88
	fimA-R	CTGACCAACGAGAACCCACT	
	16S rRNA-F	TGACACTGAAGCACGAAAGC	166
	16S rRNA-R	TCCTTGAGTTTCACCGTTGC	
P. intermedia	*inpA*-F	TTCACTGCCGAACAAGATATGG	234
	inpA-R	ATTCACACAAGGAGGTCTCTCA	
	16S rRNA-F	TGACGTGGACCAAAGATTCA	219
	16S rRNA-R	TCAATCCTGCACGCTACTTG	

2.10. Data evaluation and statistical analysis

All experiments were performed in triplicate. One-way analysis of variance with Tukey's post hoc test was used to reveal significant differences for examinations. The results are reported as mean ± standard deviation (SD) and P values < 0.05 were considered significant. The genes expression levels are shown as n-fold differences relative to the calibrator. Changes in expression levels of the target genes were significant if the variation was > 2-fold.

3. Results

3.1. Confirmation of synthesized GQD-Cur

The SEM image of GQD-Cur revealed round-shaped Cur-encapsulated GQD composites with an average size of 10 nm (Fig. 1a). Additionally, the particle size of GQD-Cur was tested by DLS as shown in Fig. 1b. It was found that the GQD-Cur size was in the range of 1–10 nm. FTIR spectra demonstrated that GQD-Cur showed stretching vibrations of O—H at 3500 cm^{-1}, C═O at 1735 cm^{-1}, and a very weak peak related to C—O—C at 1065 cm^{-1} (Fig. 1c). In addition, the crystalline structure of GQD-Cur was studied by XRD. The XRD pattern of GQD-Cur (Fig. 1d) showed a peak at $2\theta = 21^{\circ}$. According to the result of UV–Vis spectra of GQD-Cur presented in Fig. 1e, GQD-Cur had a broad absorption from 400 to 500 nm with a maximum absorption peak at ~ 430 nm, which could contribute to its photodynamic effect under blue LED. In the UV–vis spectra presented in Fig. 1f, GQD-Cur exhibited one typical absorption peak at 230 nm with a small absorption tail that extended to 350 nm. The aforementioned characterizations confirmed that GQD-Cur was successfully synthesized.

3.2. In vitro cytotoxicity of GQD-Cur

It was crucial to examine the sensitivity of eukaryotic cells to synthesized GQD-Cur. Subsequently, HuGu cells were used to evaluate the cytotoxicity of GQD-Cur. The cytotoxicity of HuGu non-targeted GQD-Cur and HuGu-targeting GQD-Cur was evaluated, and negligible cytotoxicity was exhibited against HuGu cells, with > 90% cell viability, suggesting that current synthesized GQD-Cur exhibited low toxicity to the cells and good biocompatibility with the host.

3.3. Antibacterial and anti-biofilm effects of photoexcited GQD-Cur

According to Table 2, GQD + blue LED, Cur + blue LED, and photoexcited CUR-GQD using blue LED considerably reduced the cell viability of mixed perio-pathogens ($P < 0.05$). The results revealed that GQD + blue LED, Cur + blue LED, and GQD-Cur + blue LED significantly reduced the colony counts of mixed perio-pathogens to 73.1%, 82.2% and 93% compared to the control group, respectively ($P < 0.05$; Fig. 2a). It should be noted that Cur, GQD, radiation alone, and GQD-Cur caused no significant CFU/mL reduction (9.8%, 12.3%, 12.5%, and 20.4%, respectively) in mixed perio-pathogens.

Evaluation of biofilm degradation by statistical analysis revealed a marked reduction in biofilm forms of mixed perio-pathogens in GQD + blue LED, Cur + blue LED, and GQD-Cur + blue LED groups ($P < 0.05$) (Table 2). The biofilm reduction percentage of GQD + blue LED, Cur + blue LED, and GQD-Cur + blue LED was 56.4%, 61.3% and 76%, respectively ($P < 0.05$; Fig. 2b), while there was no significant reduction in the formation of perio-pathogens mixed biofilms in GQD, Cur, GQD-Cur, and blue LED alone ($P > 0.05$).

3.4. ROS production by photoexcited GQD-Cur

Our results demonstrated a significant concentration-dependent increase in the DCFH-DA fluorescence excited GQD-Cur compared to the control group, indicating the generation of ROS. Fig. 3 shows the ROS generation of perio-pathogens mixed cells treated with GQD-Cur-aPDT (6.25–100 u g/mL of GQD-Cur irradiated with 60–420 J/cm^2 of blue LED). GQD-Cur-aPDT produced ROS in a dose-dependent manner, i.e. the fluorescence intensity of DCFH-DA was 1.81 ± 0.12 at 6.25 ug/mL of GQD-Cur irradiated with 60–80 J/cm^2 of blue LED and 21.08 at 100 ug/mL of GQD-Cur irradiated with 300–420 J/cm^2 of blue LED.

3.5. Pathogenic genes expression profile

The qRT-PCR analysis showed that aPDT treatment with GQD-Cur markedly reduced the expression level of *A. actinomycetemcomitans rcpA* gene, *P. gingivalis fimA* gene, and *P. intermedia inpA* gene by 8.1, 9.6, and 11.8 folds, respectively ($P < 0.05$). Moreover, there was a statistically significant reduction in the expression of above genes following GQD-Cur + blue LED compared to Cur + blue LED ($P < 0.05$). On the other hand, according to results, there was no significant fold decrease in *rcpA*, *fimA*, and *inpA* genes expression following treatment with GQD, Cur, GQD-Cur, and blue LED alone compared to the control group ($P > 0.05$). After treatment with GQD-Cur + blue LED and Cur + blue LED, the expression of *rcpA*, *fimA*, and *inpA* genes decreased significantly compared to treatment with GQD, Cur, GQD-Cur, and blue LED alone ($P > 0.05$).

4. Discussion

Drug release rate is very critical for a drug delivery system. As predicted, the derivative-based approach in the infection site provided favorably enhanced the therapeutic efficiency, whereby the burst and continual release of antimicrobial agents from derivative-based complexes effectively killed microbial cells and inhibited infection

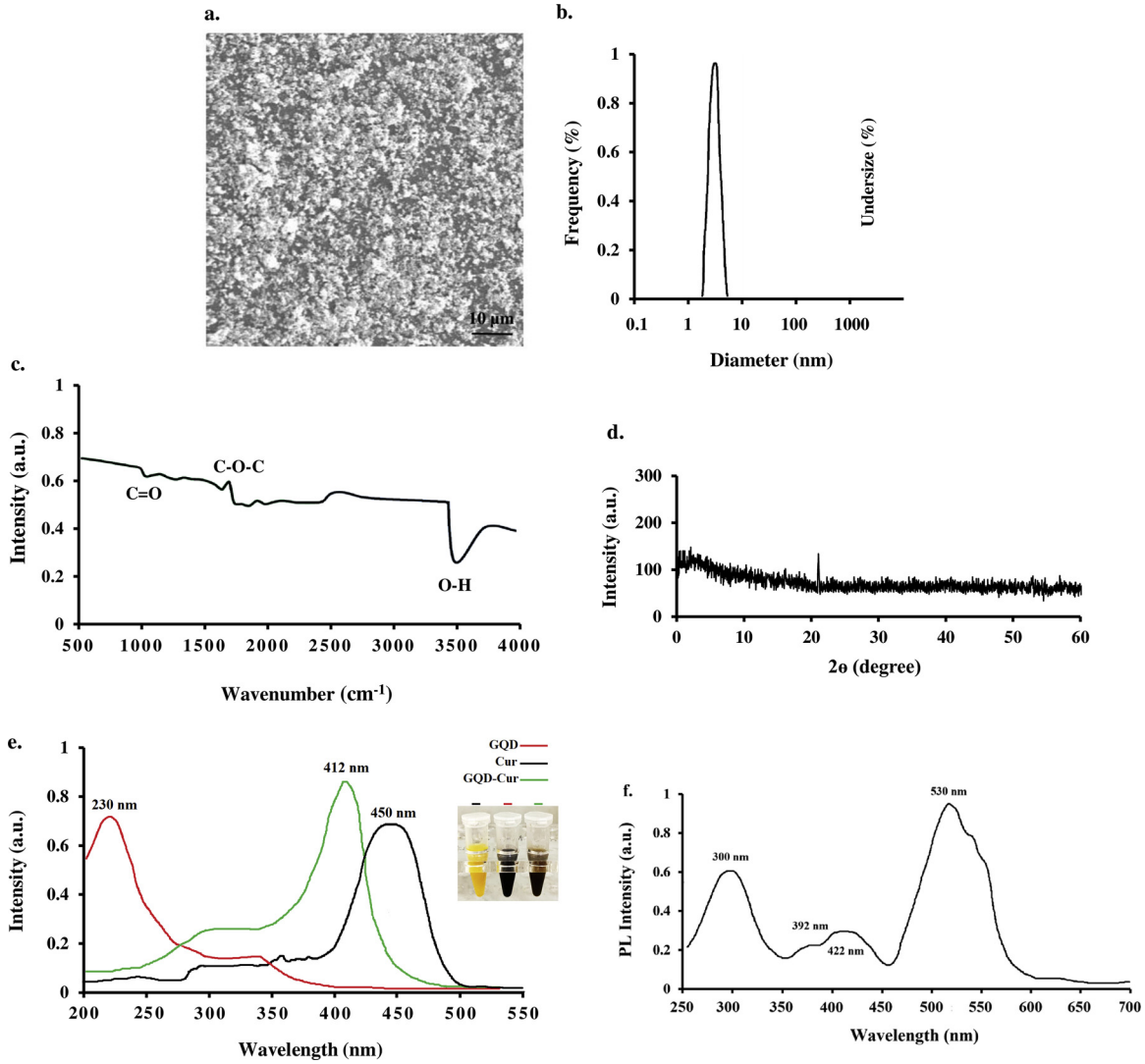

Fig. 1. Characterization of GQD-Cur: a) Representative scanning electron micrographs of synthesized GQD-Cur (scale bar represents 10 µm), b) DLS measurement of GQD-Cur, c) FTIR spectra of synthesized GQD-Cur, d) XRD pattern of GQD-Cur e) UV–vis spectra of synthesized GQD-Cur: Photoluminescence spectra of GQD-Cur; f) UV–vis spectra of synthesized GQD-Cur: Absorption spectra of GQD-Cur solution.

progression. Graphene derivative-based curcumin-complexes were investigated in various environments by altering the solution pH. In vitro experiments revealed that Cur molecules stacked on GQD remained stable in neutral buffers in which about 9.8% Cur was released from GQD at pH = 7.5 in 24 h. In sharp contrast, more CUR (as much as 85%) was readily released from GQD after 24 h at pH = 5 [27]. Song et al [28] found a rapid release of about 30% of the encapsulated doxorubicin hydrochloride (DOX), a bioprobe for tumor imaging, in the cavity of the vesicle at pH = 7.4 by NIR laser irradiation at 808 nm with a power density of 0.25 W/cm2 due to photothermal heating and disruption of the vesicle. However, their results showed that no DOX was further released post-irradiation over time, indicating that the released DOX was from the cavity of the hybrid vesicle and not from the rGO surface. Subsequently, the DOX on the rGO surface (over 80%) was

Table 2
Effects of different treatment on the viability and biofilm forms of mixed perio-pathogens.

Groups	Microbial viability assay			Biofilm assay		
	Mean of CFU/mL ± SD[a]	% of reduction	P value	Mean of OD 570 nm ± SD	% of reduction	P value
Control	3.41 ± 0.09 ×10^5	–	–	3.28 ± 0.06	–	–
Cur	3.07 ± 0.11 ×10^5	9.8	> 0.05	3.16 ± 0.02	3.4	> 0.05
GQD	2.99 ± 0.05 ×10^5	12.3	> 0.05	3.15 ± 0.08	3.8	> 0.05
Blue LED	2.98 ± 0.04 ×10^5	12.5	> 0.05	3.10 ± 0.05	5.2	> 0.05
Cur-GQD	2.71 ± 0.10 ×10^5	20.4	> 0.05	2.98 ± 0.06	9.0	> 0.05
GQD + Blue LED	0.84 ± 0.06 ×10^5	73.1	< 0.05	1.43 ± 0.07	56.4	< 0.05
Cur + Blue LED	0.60 ± 0.06 ×10^5	82.2	< 0.05	1.26 ± 0.03	61.3	< 0.05
Cur-GQD + Blue LED	0.23 ± 0.05 ×10^5	93	< 0.05	0.64 ± 0.07	76	< 0.05

[a] Standard deviation.

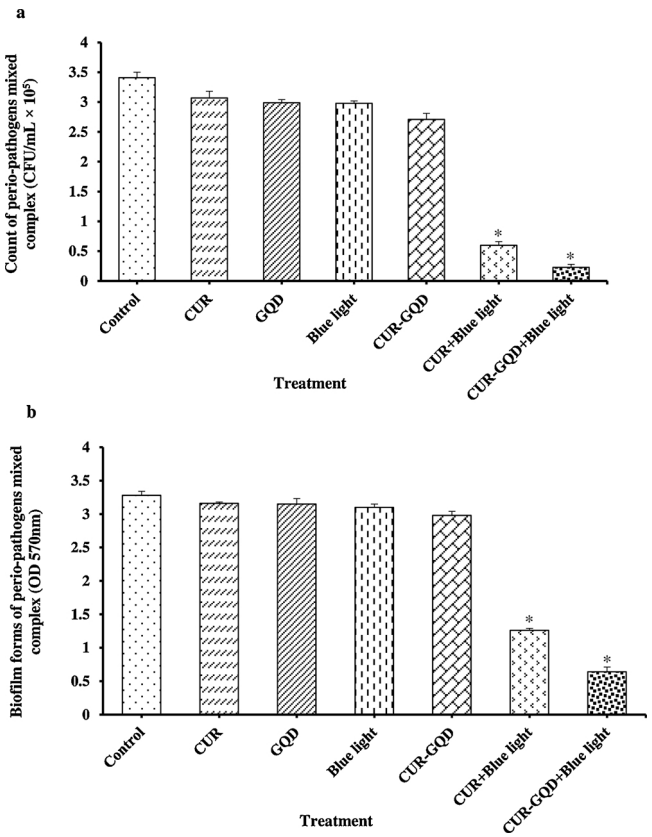

Fig. 2. a) Effect of different treatment on cell viability of mixed perio-pathogens; b) Effect of different treatment on biofilm biomass of mixed perio-pathogens. Results are represented as mean ± standard error of the mean. *Significant difference from control ($P < 0.05$).

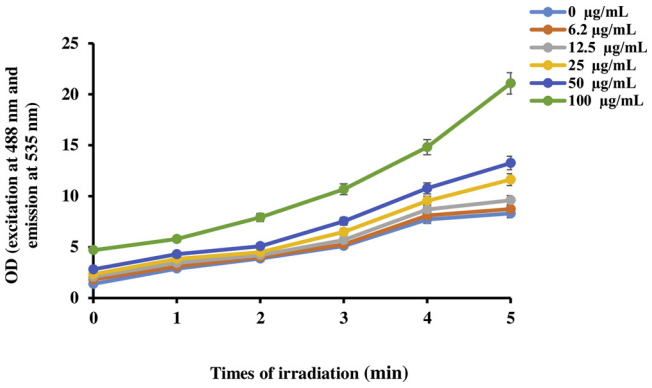

Fig. 3. Reactive oxygen species (ROS) generation of perio-pathogens mixed cells treated with different doses of GQD-Cur-aPDT. The fluorescence intensity of 2′,7′-dichlorofluoroscein (DCF), as the oxidized product of hydrolyzed 2′,7′-dichlorfluorescein-diacetate (DCFH-DA) by intracellular esterases, was measured by a fluorescence spectrophotometer at an excitation wavelength of 488 nm and at an emission wavelength of 535 nm.

released in an acidic environment (pH = 5) due to protonation and subsequent reduced interaction between DOX and rGO in acidic environments.

In the current study, a straightforward approach was used for GQD-Cur fabrication. Further investigation was performed to confirm the synthesis and high quantum yield of GQD-Cur. The biocompatibility effect of GQD-Cur was tested on HuGu cells and perio-pathogens mixed biofilms, respectively. Although this investigation demonstrated that GQD-Cur had minimal inherent cytotoxicity in fibroblast cells cultured *in vitro*, the quantum yield of our GQD-Cur was highly efficacious for aPDT targeting of perio-pathogens bacteria.

Herein, the viability of perio-pathogens was quantified through the CFU counting method, which showed nearly all GQD-Cur + blue LED-treated bacteria reduced significantly after treatment. On the other hand, photo-exited GQDs reduced the viability of perio-pathogen mixed planktonic and biofilm cultures by 73.1% and 56.4% respectively, suggesting that the effect of ROS such as $^1O_2$ produced following the activation of GQDs (as a photosensitizer) under LED irradiation. It has been shown that photo-exited GQDs exhibits a high $^1O_2$ generation yield, greater than 1.3, the highest reported for PDT photosensitizers [29].The findings of the current study were similar to the results reported by Kuo et al. [30] that used and designed the GQD as a two-photon photosensitizer coupled with two-photon excitation to achieve high efficacy against *E. coli* and methicillin-resistant *S. aureus* (MRSA). The results of their study showed that aPDT by GQD with ultra-low energy and an extremely short photoexcitation time led to almost 100% elimination of both *E. coli* and MRSA [30]. In another study, Hui et al. examined the antibacterial properties of GQD in *S. aureus, E. coli, Bacillus subtilis*, and *Pseudomonas aeruginosa.* They found that GQDs unanimously lacked antibacterial properties without light irradiation [31]. An *in vitro* study of the efficiency of QD-photosensitizer systems in killing HepG2 and HeLa cells was performed by Rakovich et al. [32]. They synthesized QD mixed with different concentrations of methylene blue. The results of their test showed a greater ROS production compared to methylene blue and irradiation alone, which is consistent with the findings of our study [32].

Despite studies investigating the effect of GQD on the planktonic form of microorganisms, there are no systematic examinations of their anti-biofilm property. This lack of information encouraged us to assess the effects of GQD anti-biofilm potency. Therefore, forasmuch as biofilm formation is an important step in the etiology of periodontal diseases in which the microbial cells become more resistant to antimicrobial agents, the intensity of the biofilm forms of mixed perio-pathogens was evaluated after photoexcited GQD-Cur. The results showed a significant reduction in the biofilm forms of mixed perio-pathogens in photoexcited GQD-Cur group compared to other groups.

The lack of information on changes in the gene expression pattern associated with biofilm formation is another factor that was addressed in this study. The *rcpA* is a virulence factor that is known to be particularly important in *A. actinomycetemcomitans* strain to form tight biofilms. It allows for interactions with host epithelial cells, which can lead to an up-regulation of biofilm-associated bacterial genes [33]. Additionally, a recent study found that *P. gingivalis* complete biofilm formation was frequently mediated by *fimA* gene of the fimbriae, which forms the filamentous structures on the bacterial cell surface [34]. *InpA* as a cysteine protease interpain in *P. intermedia* is another gene related to biofilm formation [35]. Our data indicated that photoexcited GQD-Cur could markedly reduce the gene expression of perio-pathogens compared to other groups. Also, there was no significant difference between gene expression variations of three species of mixed perio-pathogens.

Based on the scientific evidence, because GQD was considered as a photosensitizer, the ability to generate ROS was assessed. ROS is believed to play a main role in aPDT and its major products are $^1O_2$ and $O_2^{\cdot -}$ that cause microbial injury, such as DNA damage and enzyme inactivation [12,13,36–40].

The results of this study showed that in addition to the remarkable results of the antibacterial and anti-biofilm activities of photoexcited GQD-Cur, it could significantly downregulate the pathogenic genes expression profile of perio-pathogens mixed biofilms. Even though this study was conducted only *in vitro* with limited efficiency, the results revealed that GQD-Cur system was indeed superior to bare photosensitizer in terms of cell killing efficiency via aPDT.

5. Conclusion

Our findings suggest that GQD-Cur mediated aPDT might be a promising therapeutic option for treatment of perio-pathogens mixed biofilms as demonstrated by deliberate *in vitro* explorations.

The resulting non-cytotoxic photoexcited GQD-Cur exhibited a high potency of perio-pathogens suppression in planktonic and biofilm forms. In addition, by reducing the expression pattern of genes involved in the formation of biofilms, it could also reduce the progression of microbial biofilms.

Declaration of Competing Interest

The authors declare that there is no conflict of interests regarding the publication of this paper.

References

[1] C. Popova, V. Dosseva-Panova, V. Panov, Microbiology of periodontal diseases. A review, Biotechnol. Biotechnol. Equip. 27 (2013) 3754–3759.

[2] B. Benso, Virulence factors associated with *Aggregatibacter actinomycetemcomitans* and their role in promoting periodontal diseases, Virulence 8 (2017) 111–114.

[3] K.Y. How, K.P. Song, K.G. Chan, *Porphyromonas gingivalis*: an overview of periodontopathic pathogen below the gum line, Front. Microbiol. 7 (2016) 53.

[4] M. Pourhajibagher, A. Monzavi, N. Chiniforush, M.M. Monzavi, S. Sobhani, S. Shahabi, et al., Real-time quantitative reverse transcription-PCR analysis of expression stability of *Aggregatibacter actinomycetemcomitans* fimbria-associated gene in response to photodynamic therapy, Photodiagn. Photodyn. Ther. 18 (2017) 78–82.

[5] M. Pourhajibagher, N. Chiniforush, S. Shahabi, S. Sobhani, M.M. Monzavi, A. Monzavi, et al., Monitoring gene expression of *rcpA* from *Aggregatibacter actinomycetemcomitans* versus antimicrobial photodynamic therapy by relative quantitative real-time PCR, Photodiagn. Photodyn. Ther. 19 (2017) 51–55.

[6] M. Pourhajibagher, N. Chiniforush, R. Ghorbanzadeh, A. Bahador, Photo-activated disinfection based on indocyanine green against cell viability and biofilm formation of *Porphyromonas gingivalis*, Photodiagn. Photodyn. Ther. 17 (2017) 61–64.

[7] L.N. Dovigo, A.C. Pavarina, J.C. Carmello, A.L. Machado, I.L. Brunetti, V.S. Bagnato, Susceptibility of clinical isolates of Candida to photodynamic effects of curcumin, Lasers Surg. Med. 43 (2011) 927–934.

[8] L.N. Dovigo, A.C. Pavarina, A.P. Ribeiro, I.L. Brunetti, C.A. Costa, D.P. Jacomassi, et al., Investigation of the photodynamic effects of curcumin against Candida albicans, Photochem. Photobiol. 87 (2011) 895–903.

[9] G. Pileggi, J.C. Wataha, M. Girard, I. Grad, J. Schrenzel, N. Lange, et al., Blue light-mediated inactivation of Enterococcus faecalis in vitro, Photodiagn. Photodyn. Ther. 10 (2013) 134–140.

[10] M.A. Paschoal, L. Santos–Pinto, M. Lin, S. Duarte, Streptococcus mutans photoinactivation by combination of short exposure of a broad-spectrum visible lightand low concentrations of photosensitizers, Photomed. Laser Surg. 32 (2014) 175–180.

[11] N.C. Arau´jo, C.R. Fontana, V.S. Bagnato, M.E. Gerbi, Photodynamic antimicrobial therapy of curcumin in biofilms and carious dentine, Lasers Med. Sci. 29 (2014) 629–635.

[12] D. Zhang, L. Wen, R. Huang, H. Wang, X. Hu, D. Xing, Mitochondrial specific photodynamic therapy by rare-earth nanoparticles mediated near-infrared graphene quantum dots, Biomaterials 153 (2018) 14–26.

[13] F. Wo, R. Xu, Y. Shao, Z. Zhang, M. Chu, D. Shi, et al., A multimodal system with synergistic effects of magneto-mechanical, photothermal, photodynamic and chemo therapies of cancer in Graphene-Quantum Dot-coated hollow magnetic nanospheres, Theranostics 6 (2016) 485–500.

[14] M. Pourhajibagher, R. Ghorbanzadeh, S. Parker, N. Chiniforush, A. Bahador, The evaluation of cultivable microbiota profile in patients with secondary endodontic infection before and after photo-activated disinfection, Photodiagn. Photodyn. Ther. 18 (2017) 198–203.

[15] M.R. Hamblin, T. Hasan, Photodynamic therapy: a new antimicrobial approach to infectious disease? Photochem. Photobiol. Sci. 3 (2004) 436–450.

[16] T. Dai, G.P. Tegos, T. Zhiyentayev, E. Mylonakis, M.R. Hamblin, Photodynamic therapy for methicillin-resistant Staphylococcus aureus infection in a mouse skin abrasion model, Lasers Surg. Med. 42 (2010) 38–44.

[17] S. Some, A.R. Gwon, E. Hwang, G.H. Bahn, Y. Yoon, Y. Kim, et al., Cancer therapy using ultrahigh hydrophobic drug-loaded graphene derivatives, Sci. Rep. 4 (2014) 6314–6320.

[18] T.A. Tabish, C.J. Scotton, D.C.J. Ferguson, L. Lin, A.V. der Veen, S. Lowry, et al., Biocompatibility and toxicity of graphene quantum dots for potential application in photodynamic therapy, Nanomedicine (Lond.) 13 (2018) 1923–1937.

[19] J.Y. Pereyra, E.A. Cuello, H.J. Salavagione, C.A. Barbero, D.F. Acevedo, E.I. Yslas, Photothermally enhanced bactericidal activity by the combined effect of NIR laser and unmodified graphene oxide against Pseudomonas aeruginosa, Photodiagn. Photodyn. Ther. 24 (2018) 36–43.

[20] M.J. Meziani, X. Dong, L. Zhu, L.P. Jones, G.E. LeCroy, F. Yang, et al., Visible-light-activated bactericidal functions of carbon "Quantum" dots, ACS Appl. Mater. Interfaces 8 (2016) 10761–10766.

[21] B.Z. Ristic, M.M. Milenkovic, I.R. Dakic, B.M. Todorovic-Markovic, M.S. Milosavljevic, M.D. Budimir, et al., Photodynamic antibacterial effect of graphene quantum dots, Biomaterials 35 (2014) 4428–4435.

[22] X. Dong, A.E. Bond, N. Pan, M. Coleman, Y. Tang, Y.P. Sun, et al., Synergistic photoactivated antimicrobial effects of carbon dots combined with dye photosensitizers, Int. J. Nanomed. 13 (2018) 8025–8035.

[23] E. Gholibegloo, A. Karbasi, M. Pourhajibagher, N. Chiniforush, A. Ramazani, T. Akbari, et al., Carnosine-graphene oxide conjugates decorated with hydroxyapatite as promising nanocarrier for ICG loading with enhanced antibacterial effects in photodynamic therapy against *Streptococcus mutans*, J. Photochem. Photobiol. B 181 (2018) 14–22.

[24] R.V. Nair, R.T. Thomas, V. Sankar, H. Muhammad, M. Dong, S. Pillai, Rapid, acid-free synthesis of high-quality graphene quantum dots for aggregation induced sensing of metal ions and bioimaging, ACS Omega 2 (2017) 8051–8061.

[25] S. Dwivedi, R. Wahab, F. Khan, Y.K. Mishra, J. Musarrat, A.A. Al-Khedhairy, Reactive oxygen species mediated bacterial biofilm inhibition via zinc oxide nanoparticles and their statistical determination, PLoS One 9 (2014) 111289.

[26] L. Beytollahi, M. Pourhajibagher, N. Chiniforush, R. Ghorbanzadeh, R. Raoofian, B. Pourakbari, et al., The efficacy of photodynamic and photothermal therapy on biofilm formation of *Streptococcus mutans*: an in vitro study, Photodiagn. Photodyn. Ther. 17 (2017) 56–60.

[27] S. Some, A.R. Gwon, E. Hwang, G.H. Bahn, Y. Yoon, Y. Kim, et al., Cancer therapy using ultrahigh hydrophobic drug-loaded graphene derivatives, Sci. Rep. 4 (September) (2014) 1–14, https://doi.org/10.1038/srep06314 6314.

[28] J. Song, X. Yang, O. Jacobson, L. Lin, P. Huang, G. Niu, et al., Sequential drug release and enhanced photothermal and photoacoustic effect of hybrid reduced graphene oxide-loaded ultrasmall gold nanorod vesicles for cancer therapy, ACS Nano 22 (2015) 9199–9209.

[29] J. Ge, M. Lan, B. Zhou, W. Liu, L. Guo, H. Wang, et al., A graphene quantum dot photodynamic therapy agent with high singlet oxygen generation, Nat. Commun. 5 (4596) (2014) 1–8, https://doi.org/10.1038/ncomms5596.

[30] W.S. Kuo, C.Y. Chang, H.H. Chen, C.L. Hsu, J.Y. Wang, H.F. Kao, et al., Two-photon photoexcited photodynamic therapy and contrast agent with antimicrobial graphene quantum dots, ACS Appl. Mater. Interfaces 8 (2016) 30467–30474.

[31] L. Hui, J. Huang, G. Chen, Y. Zhu, L. Yang, Antibacterial property of graphene quantum dots (Both source material and bacterial shape matter), ACS Appl. Mater. Interfaces 8 (2016) 20–25.

[32] A. Rakovich, T. Rakovich, V. Kelly, V. Lesnyak, A. Eychmüller, Y.P. Rakovich, et al., Photosensitizer methylene blue-semiconductor nanocrystals hybrid system for photodynamic therapy, J. Nanosci. Nanotechnol. 10 (2010) 2656–2662.

[33] V. Zijnge, T. Kieselbach, J. Oscarsson, Proteomics of protein secretion by *Aggregatibacter actinomycetemcomitans*, PLoS One 7 (2012) e41662.

[34] M. Krishnan, P. Krishnan, S.C. Chandrasekaran, Detection of Porphyromonas gingivalis fimA type I genotype in gingivitis by real-time PCR-a pilot study, J. Clin. Diagn. Res. 10 (2016) 32–35.

[35] D.P. Byrne, J. Potempa, T. Olczak, J.W. Smalley, Evidence of mutualism between two periodontal pathogens: co-operative haem acquisition by the HmuY haemophore of *Porphyromonas gingivalis* and the cysteine protease interpain A (InpA) of *Prevotella intermedia*, Mol. Oral Microbiol. 28 (June (3)) (2013) 219–229.

[36] Y. Zhang, C. Yang, D. Yang, Z. Shao, Y. Hu, J. Chen, et al., Reduction of graphene oxide quantum dots to enhance the yield of reactive oxygen species for photodynamic therapy, Phys. Chem. Chem. Phys. 20 (2018) 17262–17267.

[37] Y. Liu, Y. Xu, X. Geng, Y. Huo, D. Chen, K. Sun, et al., Synergistic targeting and efficient photodynamic therapy based on Graphene Oxide Quantum Dot-upconversion nanocrystal hybrid nanoparticles, Small. 14 (2018) e1800293.

[38] N. Zhang, J. Hou, S. Chen, C. Xiong, H. Liu, Y. Jin, et al., Rapidly probing antibacterial activity of graphene oxide by mass spectrometry-based metabolite fingerprinting, Sci. Rep. 6 (2016) 28045.

[39] M. Di Giulio, R. Zappacosta, S. Di Lodovico, E. Di Campli, G. Siani, A. Fontana, et al., Antimicrobial and antibiofilm efficacy of graphene oxide against chronic wound microorganisms, Antimicrob. Agents Chemother. 62 (2018) e00547–18.

[40] R. Yu, S. Zheng, Poly(acrylic acid)-grafted poly(N-isopropyl acrylamide) networks: preparation, characterization and hydrogel behavior, J. Biomater. Sci. Polym. Ed. 22 (2011) 2305–2324.